

Heat Generation/Absorption effects on Magneto-Williamson Nanofluidflow with Heat and Mass Fluxes

¹G.Venkataramanaiah, ²Dr M.SreedharBabu, ³M.Lavanya
¹Research scholar, ²Asst.professor, ³Research scholar,
 Dept. of Applied Mathematics,
 Yogi Vemana University, Kadapa, Andhra Pradesh, India.

Abstract - This study investigates the effect of the nano particle effect on magnetohydrodynamic boundary layer flow over a stretching surface in the presence of heat generation or absorption with heat and mass fluxes. The governing partial differential equations are transformed to a system of ordinary differential equations and solved numerically using fifth order Runge-Kutta method integration scheme and Matlab bvp4c solver. The effects of the Non-Newtonian Williamson parameter, Prandtl number, Lewis number, the diffusivity ratio parameter, heat capacities ratio parameter, heat generation or absorption parameter, Schmidt number on the fluid properties as well as on the skin friction, heat and mass transfer rates are determined and shown graphically

Keywords - MHD, nanoparticle, heat generation/absorption, Williamson fluid model, heat and mass fluxes.

1. INTRODUCTION

Investigations of magnetohydrodynamic (MHD) boundary layer flow and heat transfer of viscous fluids over a flat sheet are important in many manufacturing processes, such as polymer extrusion, drawing of copper wires, continuous stretching of plastic films and artificial fibers, hot rolling, wire drawing, glass-fiber, metal extrusion, and metal spinning. Among these studies, Sakiadis [1], initiated the study of the boundary layer flow over a stretched surface moving with a constant velocity and formulated a boundary-layer equation for two-dimensional and axisymmetric flows. Shateyi and Prakash [2] investigated the magnetohydrodynamic boundary layer flow of a nanofluid over a moving surface in the presence of thermal radiation. Bhaskar Reddy et al. [3] studied the influence of variable thermal conductivity and partial velocity slip on hydromagnetic two-dimensional boundary layer flow of a nanofluid with Cu nanoparticles over a stretching sheet with convective boundary condition and also concluded that the velocity decreases as the magnetic parameter increases. Mukhopadhyay et al. [4] investigated MHD flow and heat transfer past a porous stretching non-isothermal surface in porous medium with variable free stream temperature. Krishnamurthy et al. [5] investigated the radiation and chemical reaction effects on the steady boundary layer flow of MHD Williamson fluid through porous medium toward a horizontal linearly stretching sheet in the presence of nanoparticles and concluded that magnetic parameter decreases the velocity and also causes increase in its temperature. El-Amin [6] investigated free convection with mass transfer flow for a micropolar fluid bounded by a vertical infinite surface under the action of a transverse magnetic field. Mohammed Ibrahim et al. [7] investigated the radiation and mass transfer effects on MHD oscillatory flow in a channel filled with porous medium in the presence of chemical reaction. Nadeem and Hussain [8] studied the flow and heat transfer analysis of Williamson nanofluid.

Makinde [9] studied the hydromagnetic mixed convection flow of an incompressible viscous electrically conducting fluid and mass transfer over a vertical porous plate with constant heat flux embedded in a porous medium. Bachok and Ishak [10] investigated the magnetohydrodynamic (MHD) mixed convection stagnation point flow towards a vertical surface immersed in an incompressible micropolar fluid with prescribed wall heat flux solved numerically by a finite-difference method. Devi et al. [11] studied the dissipation effects on MHD nonlinear flow and heat transfer past a porous surface with prescribed heat flux. Qasim et al. [12] studied the MHD boundary layer slip flow and heat transfer of ferrofluid along a stretching cylinder with prescribed heat flux.

Das et al. [13] investigated the MHD boundary layer slip flow and heat transfer of nanofluid past a vertical stretching sheet with non-uniform heat generation/absorption. Rajotia and Jat [14] studied the three dimensional MHD boundary layer flow and heat transfer due to an axisymmetric shrinking sheet with viscous dissipation and heat generation/absorption. Megahed [15] analyzed the boundary layer flow and heat transfer for an electrically conducting Casson fluid over a permeable stretching surface with second-order slip velocity model and thermal slip conditions in the presence of internal heat generation/absorption and thermal radiation using shooting method. Abd El-Aziz and Nabil [16] investigated the effect of time-dependent heat source/sink on heat transfer characteristics of the unsteady mixed convection flow over an exponentially stretching surface. Dessie and Kishan [17] investigated the MHD boundary layer flow and heat transfer of a fluid with variable viscosity through a porous medium towards a stretching sheet by taking in to the effects of viscous dissipation in presence of heat source/sink and concluded that due to the internal heat sink the thermal boundary layer increases, whereas it decreases with heat source. Hitesh Kumar [18] studied the effects of radiation and heat sink over a stretching surface in the presence of a transverse magnetic field on two-dimensional boundary layer steady flow and heat transfer of a viscous incompressible fluid. Basiri Parsa et al. [19] investigated the MHD

boundary-layer flow over a stretching surface with internal heat generation or absorption. El-Amin et al. [20] analyzed the free convection with mass transfer flow for a micropolar fluid bounded by a vertical infinite surface with an exponentially decaying heat generation, under the action of a transverse magnetic field. Sharma et al [21] investigated the micropolar fluid flow and heat transfer along a semi-infinite vertical porous moving plate including the effect of viscous heating and in the presence of a magnetic field applied transversely to the direction of the flow. Takhar et al. [22] investigated the combined buoyancy effects of thermal and mass diffusion on MHD convection flow in the presence of Hall currents with variable suction and heat generation. Chamkha [23] studied the hydromagnetic flow and heat and mass transfer over a permeable cylinder moving with a linear velocity in the presence of heat generation/absorption, chemical reaction, suction/injection effects and uniform transverse magnetic field. Kinyanjui et al. [24] investigated the magnetohydrodynamic free convection heat and mass transfer of a heat generating fluid past an impulsively started infinite vertical porous plate with Hall current and radiation absorption. Gangadhar [25] investigated the effects of internal heat generation and viscous dissipation on boundary layer flow over a vertical plate with a convective surface boundary condition and concluded that local skin friction coefficient increases and local Nusselt number coefficient decreases with an increase in both Eckert number and local heat generation parameter. Gangadhar [26] investigated the radiation, heat generation viscous dissipation and magnetohydrodynamic effects on the laminar boundary layer about a flat-plate in a uniform stream of fluid (Blasius flow), and about a moving plate in a quiescent ambient fluid (Sakiadis flow) both under a convective surface boundary condition.

However, the interactions of magnetohydrodynamic boundary layer flow on heat transfer of Williamson nanofluid flow in the presence of heat generation or absorption and heat and mass fluxes. The governing boundary layer equations have been transformed to a two-point boundary value problem in similarity variables and the resultant problem is solved numerically using the fourth order Runge-Kutta method along with shooting technique. The effects of various governing parameters on the fluid velocity, temperature, nanoparticle volume fraction, reduced Nusselt number and nanoparticle volume fraction gradient are shown in figures and analyzed in detail.

2. MATHEMATICAL FORMULATION

Let us consider the two-dimensional steady flow of an incompressible nano Williamson fluid over a stretching surface. A uniform magnetic field is applied in the y-direction normal to the flow direction. The magnetic Reynolds number is assumed to be small so that the induced magnetic field is neglected. The plate is stretched along x-axis with a velocity Bx , where $B > 0$ is stretching parameter. Schematic diagram of the boundary layer flow over Stretching sheet is shown in Figure A.

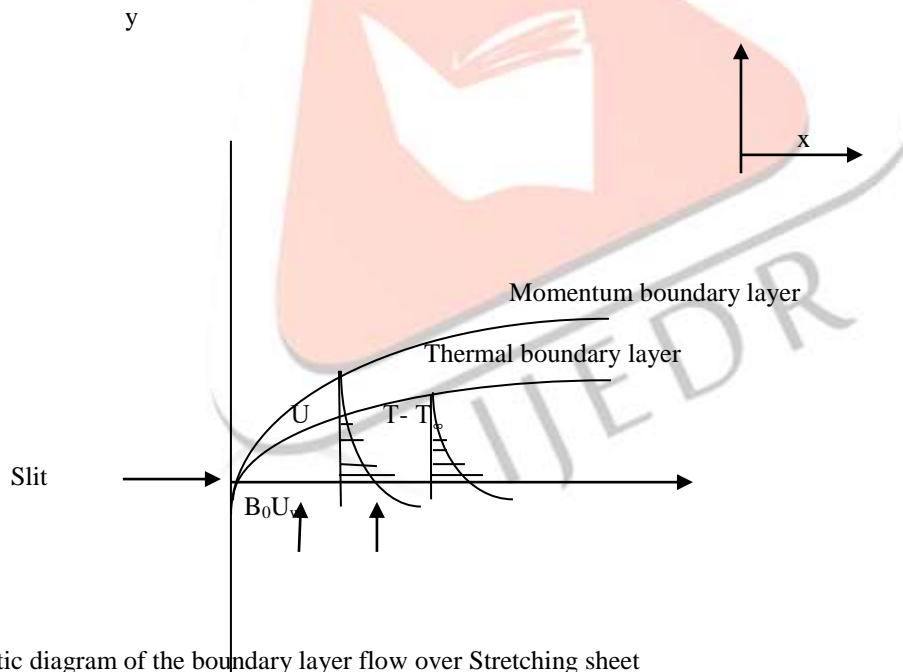


Fig.A: Schematic diagram of the boundary layer flow over Stretching sheet

The fluid velocity, temperature and nanoparticle concentration near surface are assumed to be U_w , T_w and C_w , respectively.

For Williamson fluid model is defined in (Dapra [27]) as

$$\tau = \left[\mu_0 + \frac{(\mu_0 - \mu_\infty)}{1 - \Gamma \dot{\gamma}} \right] \Lambda_1 \tag{2.1}$$

where τ is extra stress tensor, μ_0 is limiting viscosity at zero shear rate and μ_∞ is limiting viscosity at infinite shear rate,

$\Gamma > 0$ is a time constant, Λ_1 is the first Rivlin–Erickson tensor and $\dot{\gamma}$ is defined as follows:

$$\dot{\gamma} = \sqrt{\frac{1}{2}}\pi \quad (2.2)$$

$$\pi = \text{trace}(\Lambda_1^2) \quad (2.3)$$

Here we considered the case for which $\mu_\infty = 0$ and $\Gamma \dot{\gamma} < 1$. Thus Eq. (2.1) can be written as

$$\tau = \left[\frac{\mu_0}{1 - \Gamma \dot{\gamma}} \right] \Lambda_1 \quad (2.4)$$

or by using binomial expansion we get

$$\tau = \mu_0 \left[1 + \Gamma \dot{\gamma} \right] \Lambda_1 \quad (2.5)$$

The above model reduces to Newtonian for $\Gamma = 0$

The equations governing the flow are

Continuity equation

$$\frac{\partial u}{\partial x} + \frac{\partial v}{\partial y} = 0 \quad (2.6)$$

Momentum equation

$$u \frac{\partial u}{\partial x} + v \frac{\partial u}{\partial y} = \nu \frac{\partial^2 u}{\partial y^2} + \sqrt{2M} \frac{\partial u}{\partial y} \frac{\partial^2 u}{\partial y^2} - \frac{\sigma B_0^2}{\rho} u \quad (2.7)$$

Energy equation

$$u \frac{\partial T}{\partial x} + v \frac{\partial T}{\partial y} = \alpha \frac{\partial^2 T}{\partial y^2} + \frac{\rho_p c_p}{\rho c} \left[D_B \frac{\partial C}{\partial y} \frac{\partial T}{\partial y} + \frac{D_T}{T_\infty} \left(\frac{\partial T}{\partial y} \right)^2 \right] + \frac{1}{\rho c_p} q_0 (T - T_\infty) \quad (2.8)$$

Volumetric species equation

$$u \frac{\partial C}{\partial x} + v \frac{\partial C}{\partial y} = D_B \frac{\partial^2 C}{\partial y^2} + \frac{D_T}{T_\infty} \frac{\partial^2 T}{\partial y^2} \quad (2.9)$$

The boundary conditions are

$$u = U_w, v = 0, \frac{\partial T}{\partial y} = -\frac{q_w}{\alpha}, \frac{\partial C}{\partial y} = -\frac{q_m}{D_B} \text{ at } y = 0$$

$$u \rightarrow 0, T \rightarrow T_\infty, C \rightarrow C_\infty \text{ as } y \rightarrow \infty \quad (2.10)$$

Since the surface is stretched with velocity Bx , thus $U_w = Bx$ and u and v are horizontal and vertical components of velocity, ν is the kinematic viscosity, q_w, q_m are the heat and mass fluxes unit area at the surface, respectively. B_0 is the magnetic field, α is the nanofluid thermal diffusivity. ρ is nanofluid density, q_0 is the heat source/sink constant, ρc and $\rho_p c_p$ are heat capacities of nanofluid and nanoparticles, respectively, T is temperature, k is nanofluid thermal conductivity, D_B is Brownian diffusion coefficient, C is nanoparticle volumetric fraction, D_T is thermophoretic diffusion coefficient and T_∞ is the ambient fluid temperature.

In order to transform the equations (2.6) to (2.10) into a set of ordinary differential equations, the following similarity transformations and dimensionless variables are introduced.

$$\begin{aligned}
u &= Bx f'(\eta), v = -\sqrt{B\nu} f(\eta), \eta = y\sqrt{\frac{B}{\nu}} \\
\theta(\eta) &= \frac{T - T_\infty}{T_w - T_\infty}, \phi(\eta) = \frac{C - C_\infty}{C_w - C_\infty}, Pr = \frac{\nu}{\alpha}, M = \frac{\sigma B_0^2}{\rho B} \\
Le &= \frac{\alpha}{D_B}, \beta = \Gamma x \sqrt{\frac{2B^3}{\nu}}, Sc = \frac{\nu}{D_B}, Q = \frac{q_0}{B\rho c_p} \\
Nc &= \frac{\rho_p c_p (C_w - C_\infty)}{\rho c}, Nt = \frac{D_B T_\infty (C_w - C_\infty)}{D_T (T_w - T_\infty)}
\end{aligned} \tag{2.11}$$

where $f(\eta)$ is the dimensionless stream function, θ -the dimensionless temperature, ϕ - the dimensionless nanoparticle volume fraction, η -the similarity variable, M - magnetic parameter, β - the Non-Newtonian williamson parameter, Le - the Lewis number, Nc - the heat capacities ratio, Nt - the diffusivity ratio, Q -the heat generation/absorption parameter, Pr - the Prandtl number, Sc - the Schmidt number.

In view of the equation(2.11),the equations (2.7) to (2.10) transform into

$$f''' + ff'' - f'^2 + \beta f'' f''' - Mf' = 0 \tag{2.12}$$

$$\theta'' + Pr f \theta' + \frac{Nc}{Le} \theta' \phi' + \frac{Nc}{LeNt} \theta'^2 + Q\theta = 0 \tag{2.13}$$

$$\phi'' + Scf \phi' + \frac{1}{Nt} \theta'' = 0 \tag{2.15}$$

The transformed boundary conditions can be written as

$$f = 0, f' = 1, \theta' = -1, \phi' = -1 \text{ at } \eta = 0$$

$$f' \rightarrow 0, \theta \rightarrow 0, \phi \rightarrow 0 \text{ as } \eta \rightarrow \infty \tag{2.16}$$

Where the prime denote differentiation with respect to η .

If we put $\beta = 0$, our problem reduces to the one for Newtonian nano and for $D_B = D_T = 0$ in Eq. (2.8) our heat equation reduce to the classical boundary layer heat equation in the absence of heat generation/absorption.

The quantities of physical interest are the values of $f''(0)$, $1/\theta(0)$ and $1/\phi(0)$ which represent the skin friction, heat and mass transfer rates of the surface, respectively.

Where $Re = \frac{Bx^2}{\nu}$ is the local Reynolds number.

3 SOLUTION OF THE PROBLEM

The set of non-linear coupled differential Eqs. (2.12)-(2.15) subject to the boundary conditions Eq. (2.16) constitute a two-point boundary value problem. In order to solve these equations numerically we follow most efficient numerical shooting technique with fifth-order Runge-Kutta-integration scheme. In this method it is most important to choose the appropriate finite values of $\eta \rightarrow \infty$. To select η_∞ we begin with some initial guess value and solve the problem with some particular set of parameters to obtain f'', θ' and ϕ' . The solution process is repeated with another large value of η_∞ until two successive values of f'', θ' and ϕ' differ only after desired digit signifying the limit of the boundary along η . The last value of η_∞ is chosen as appropriate value of the limit $\eta \rightarrow \infty$ for that particular set of parameters. The four ordinary differential Eqs. (2.12)-(2.15) were first formulated as a set of seven first-order simultaneous equations of seven unknowns following the method of superposition [18]. Thus, we set

$$y_1 = f, y_2 = f', y_3 = f'', y_4 = \theta, y_5 = \theta', y_6 = \phi, y_7 = \phi'$$

$$y_1' = y_2, y_2' = y_3$$

$$y_1(0) = 0, y_2(0) = 1$$

$$y_3' = \frac{1}{1 + \beta y_3} (y_2^2 - y_1 y_3)$$

$$y_3(0) = \delta_1$$

$$y_4' = y_5, y_5(0) = -1$$

$$y_5' = - \left[Pr y_1 y_5 + Q y_4 + \frac{Nc}{Le} y_5 y_7 + \frac{Nc}{Le Nt} y_5^2 \right]$$

$$y_5(0) = \delta_2$$

$$y_6' = y_7, y_7(0) = -1$$

$$y_7' = - \left[Sc y_1 y_6 + \frac{1}{Nt} y_5' \right]$$

$$y_7(0) = \delta_3$$

Eqs. (2.12)-(2.15) then reduced into a system of ordinary differential equations, i.e., where δ_1, δ_2 and δ_3 are determined such that it satisfies $y_2(\infty) \rightarrow 0, y_4(\infty) \rightarrow 0$ and $y_6(\infty) \rightarrow 0$. The shooting method is used to guess δ_1, δ_2 and δ_3 until the boundary conditions $y_2(\infty) \rightarrow 0, y_4(\infty) \rightarrow 0$ and $y_6(\infty) \rightarrow 0$ are satisfied. Then the resulting differential equations can be integrated by fourth-order Runge-Kutta scheme. The above procedure is repeated until we get the results up to the desired degree of accuracy, 10^{-6}

4 RESULTS AND DISCUSSION

In order to get a clear insight of the physical problem, the velocity, temperature and nanoparticle volume fraction have been discussed by assigning numerical values to the governing parameters encountered in the problem. Numerical computations are shown from figs. 1-10.

Figs. 1(a)-(c) shows the effect of the magnetic parameter (M) on the velocity, temperature and mass volume fraction profiles. It is observed that the velocity of the fluid decreases with increases the values of M and temperature as well as mass volume fraction of the fluid increases with raising the values of M. Figs. 2(a)-(c) shows the effect of the non-Newtonian Williamson parameter (β) on the velocity, temperature and mass volume fraction profiles. It is observed that the velocity of the fluid decreases with an increase β and temperature as well as mass volume fraction of the fluid increases with raising the values of β .

The effect of Nc on temperature and mass volume fraction is shown in figs. 3(a) & 3(b). An increase in Nc the temperature of the fluid is increases and mass volume fraction initially decrease and then increase. The effect of Nb on temperature and mass volume fraction is shown in figs. 4(a) & 4(b). An increase in Nc the temperature and mass volume fraction of the fluid is decreases. The effect of heat generation/absorption (Q) on temperature and mass volume fraction is shown in figs. 5(a)&5(b). Increases in Q the temperature of the fluid are decreases as well as same results were found in mass volume fraction. The effect of the Prandtl number (Pr) on temperature is shown in fig. 6. Since the Prandtl number is the ratio of momentum diffusivity to the nanofluid thermal diffusivity. It is noticed that temperature of the fluid decreases with an increases the Prandtl number.

From fig. 7 show that the effect of Lewis number (Le) on temperature. Since Lewis number is the ratio of nanoparticle thermal diffusivity to Brownian diffusivity. It is observe that the temperature of the fluid decreases with an increase in the Lewis number. The effect of the Schmidt number (Sc) on mass volume fraction is shown in fig. 8. It is noticed that mass volume fraction of the fluid decreases with an increases the Schmidt number.

Fig. 9(a) & 9(b) shows the effects of M and β on Nusselt number and Sherwood number. From fig. 9(a) & 9(b) it is seen that both the $1/\theta(0)$ and $1/\phi(0)$ decreases with an increase M or β . The variations of Nc and Nb on local Nusselt number and local sherwood is shown in fig. 10(a) & 10(b). It is observed that the $1/\theta(0)$ increases with an increases Nb and decrease with an increasing Nc , but the $1/\phi(0)$ increases with an increase Nc or Nb . Table 1 is shows to compare our results for the viscous case in the absence of nanoparticles and viscous dissipation. These results are found to be in good agreement.

5 CONCLUSIONS

In this paper numerically investigated the nanoparticle effect on magnetohydrodynamic boundary layer flow of Williamson fluid over a stretching surface in the presence of heat generation or absorption and heat and mass fluxes. The important findings of the paper are:

- The velocity of the fluid decreases with an increase of the Non-Newtonian Williamson parameter or magnetic parameter. The fluid temperature and mass volume friction increases with the influence of non-Newtonian Williamson parameter or magnetic parameter.
- The temperature and nanoparticle volume friction enhance with the raising the values of heat generation/absorption parameter.
- Both the local Nusselt number and local Sherwood number decreases with the raising the values of non-Newtonian Williamson parameter or magnetic parameter.

GRAPHS

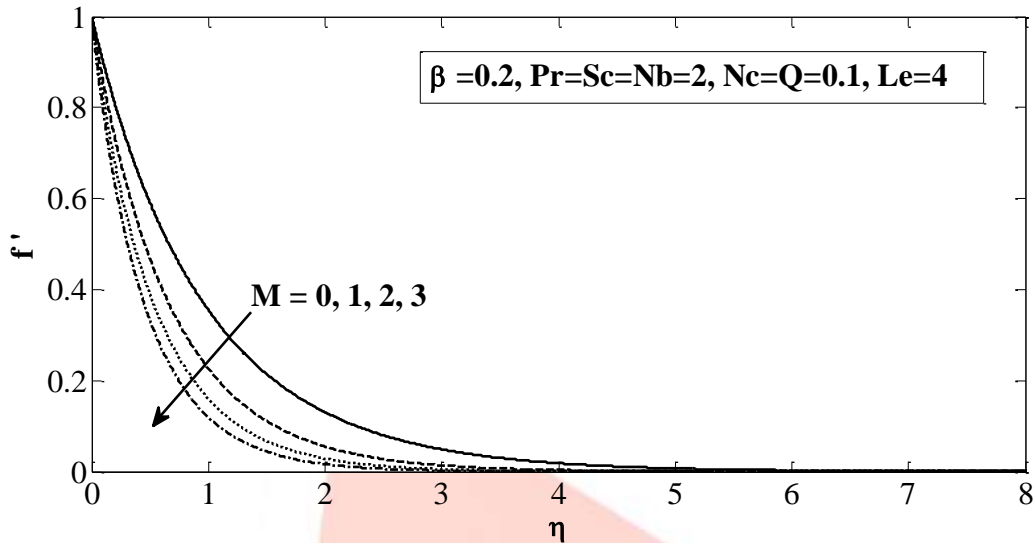


Fig.1(a) Velocity for different values of M

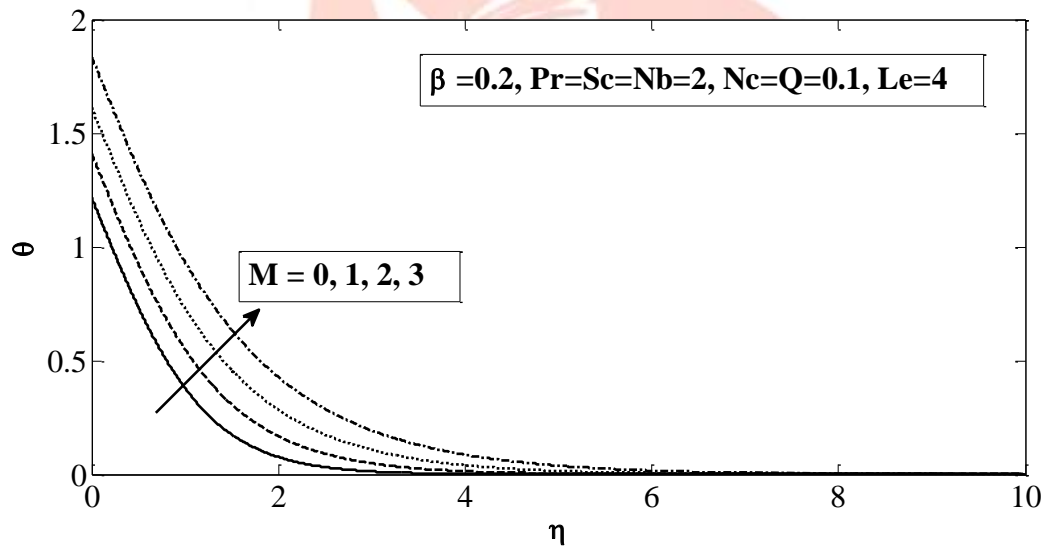


Fig.1(b) Temperature for different values of M

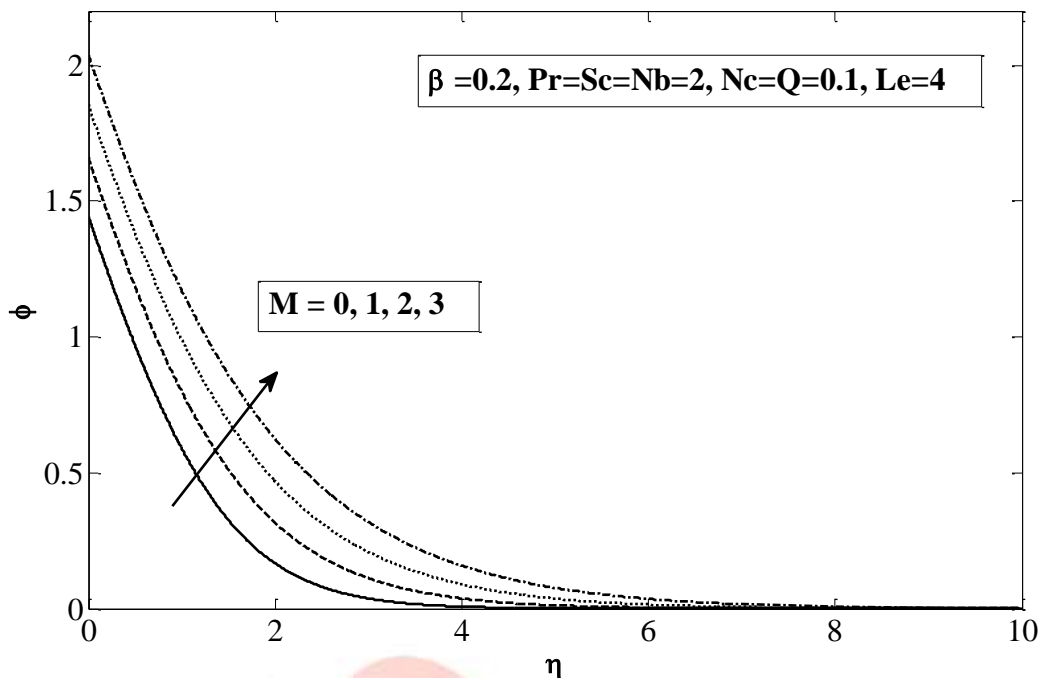


Fig.1(c) Nanoparticle volume fraction for different values of M

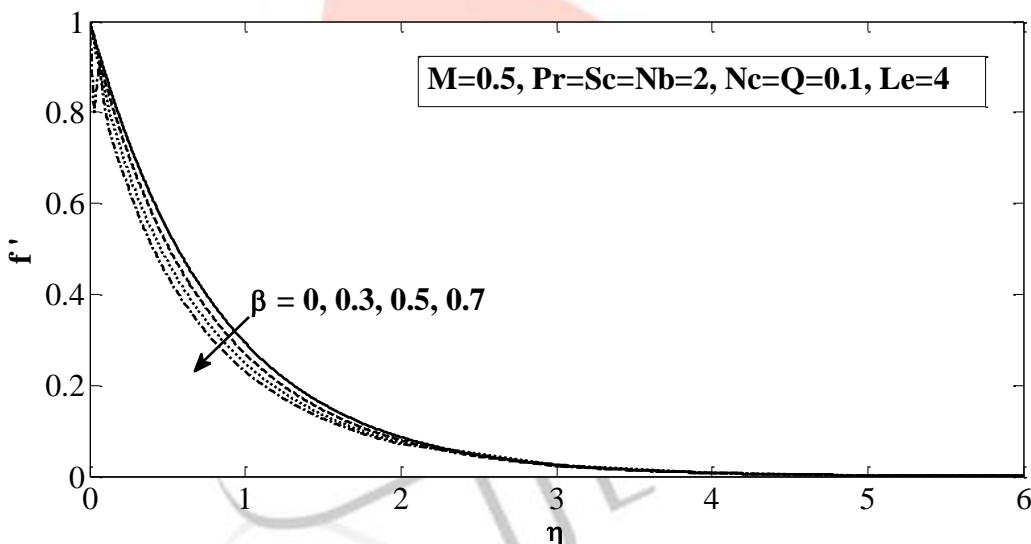


Fig.2 (a) Velocity for different values of β

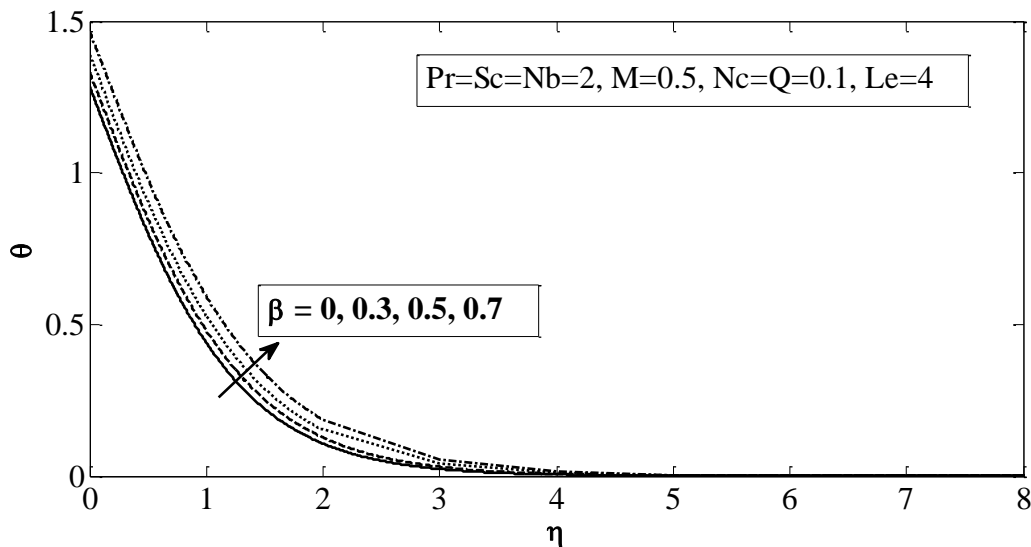


Fig.2(b) Temperature for different values of β

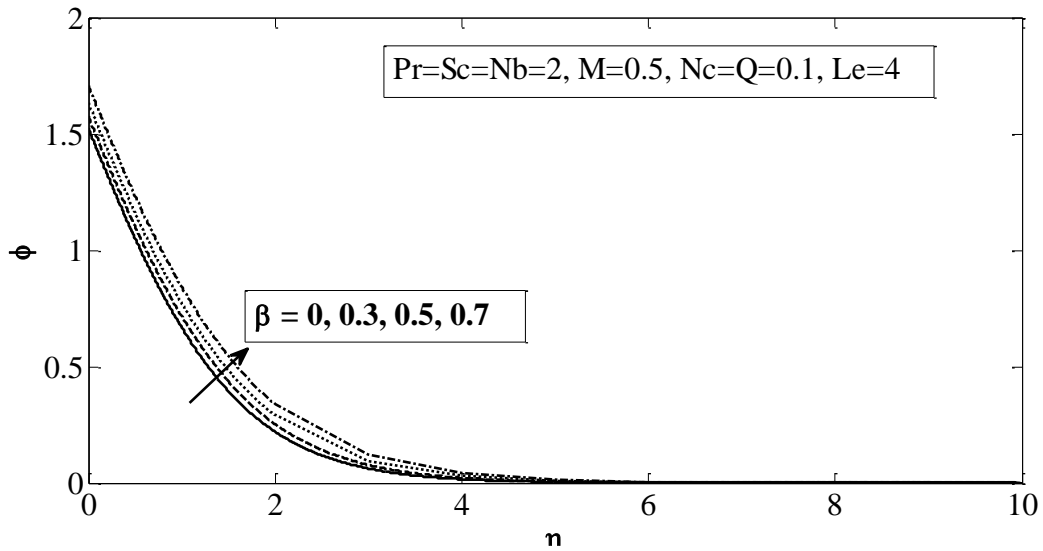


Fig.2(c) Nanoparticle volume fraction for different values of β

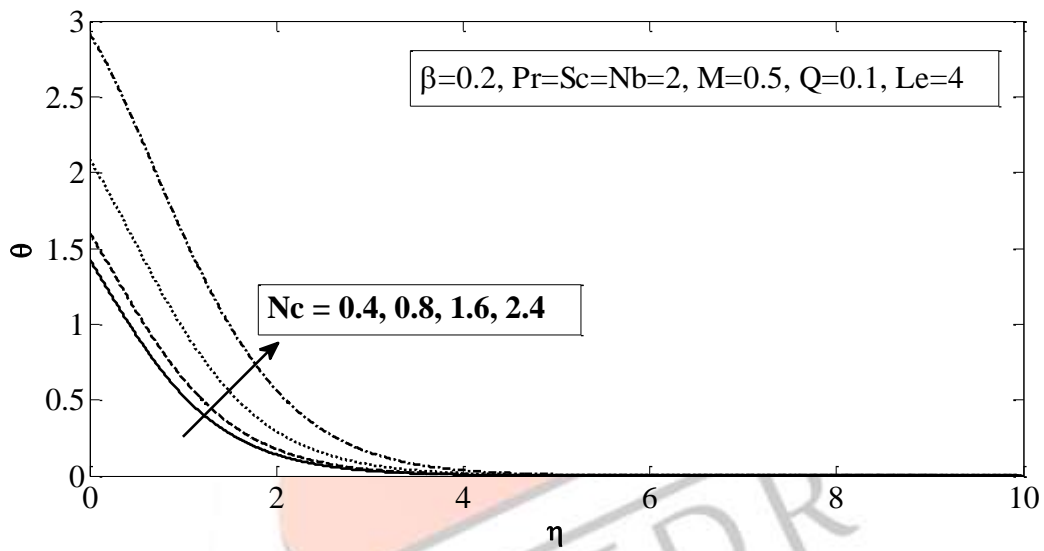


Fig.3(a) Temperature for different values of Nc

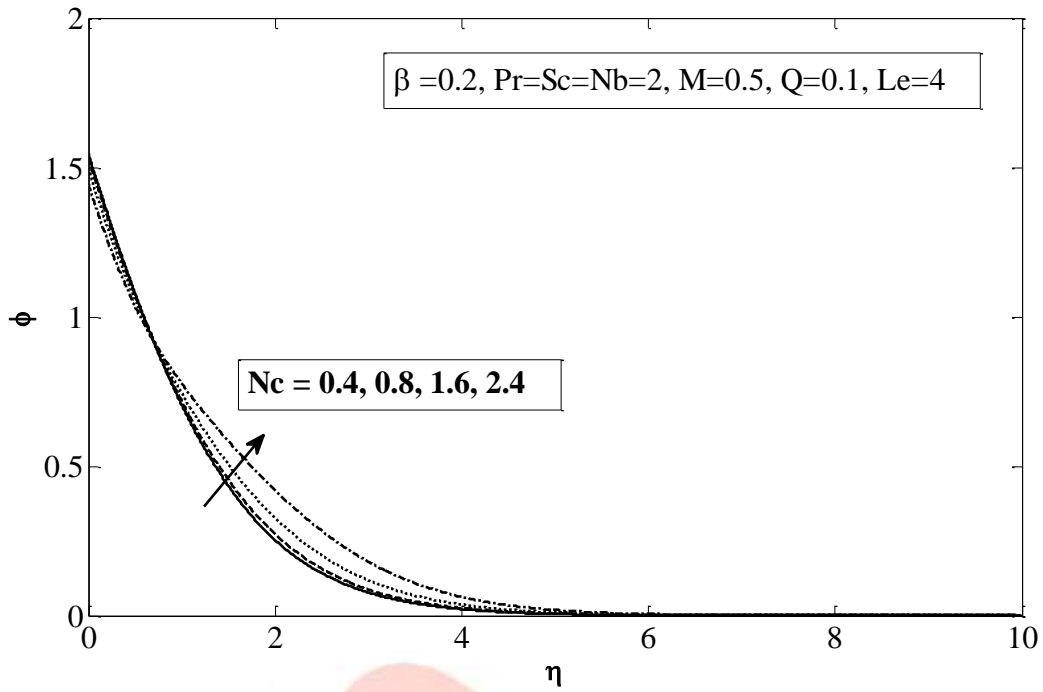


Fig.3(b) Nanoparticle volume fraction for different values of N_c

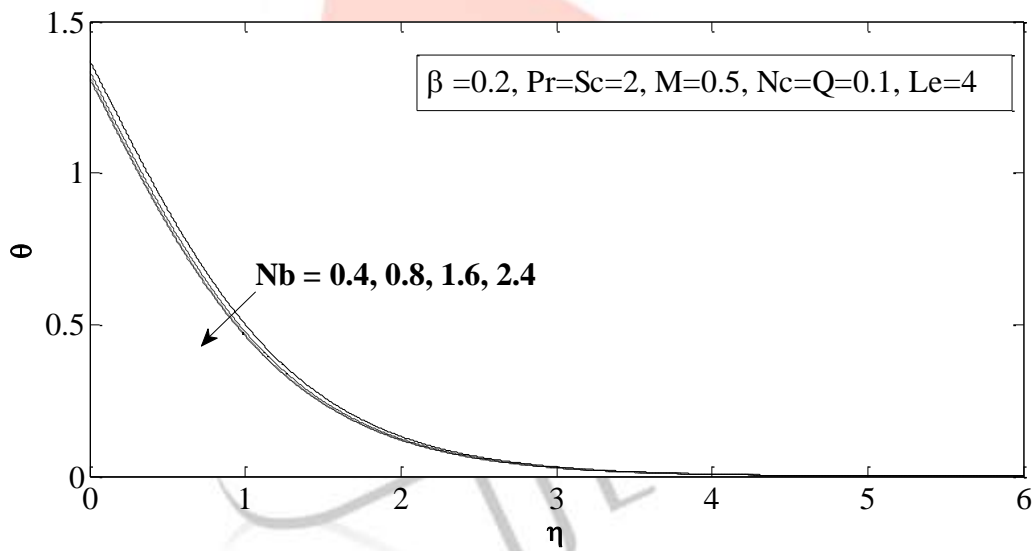


Fig.4(a) Temperature for different values of N_b

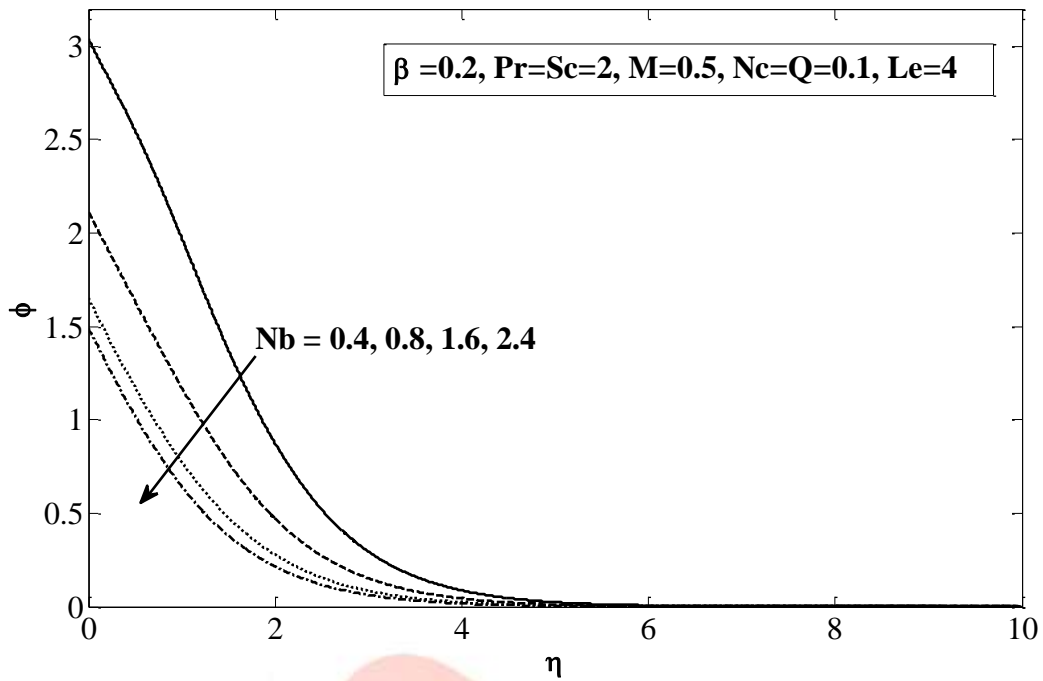


Fig.4(b) Nanoparticle volume fraction for different values of Nb

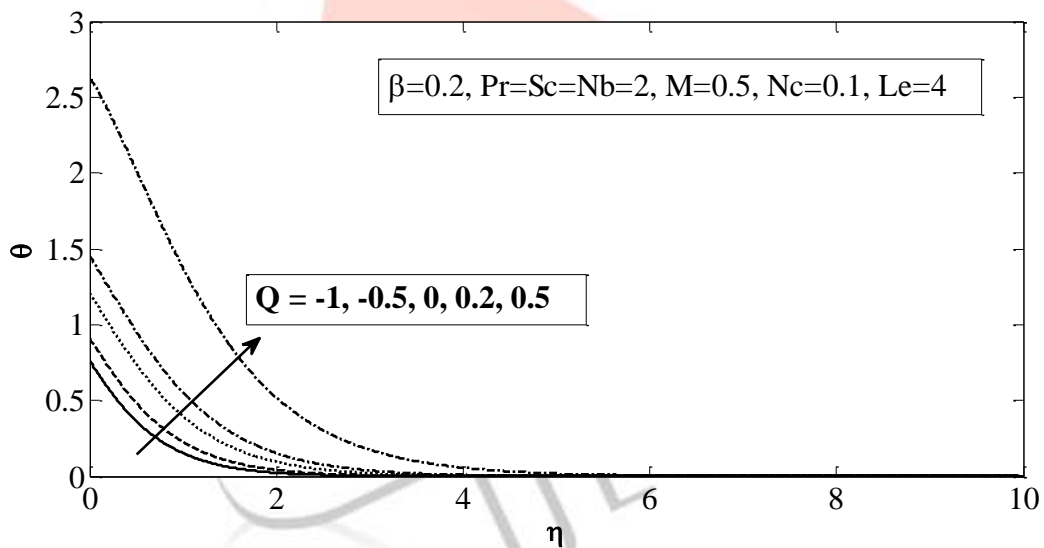


Fig.5(a) Temperature for different values of Q

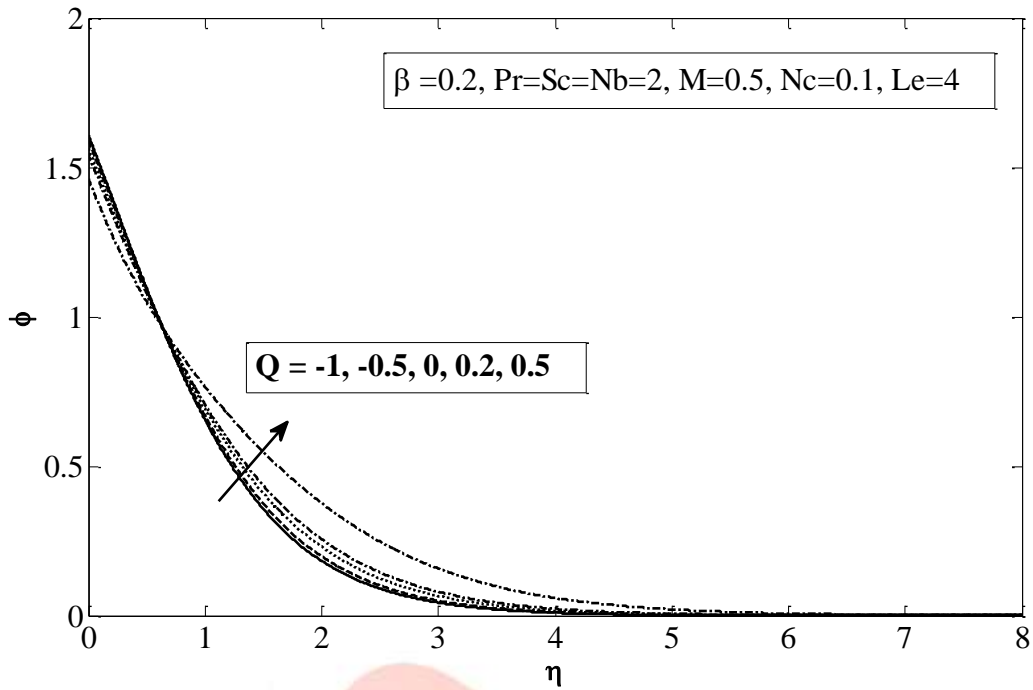


Fig.5(b) Nanoparticle volume fraction for different values of Q

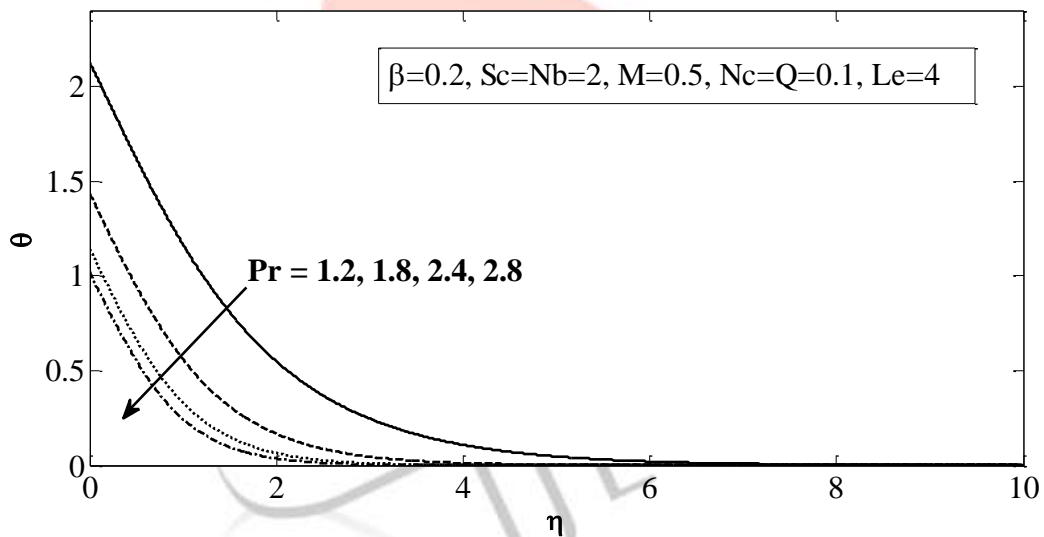


Fig.6 Temperature for different values of Pr

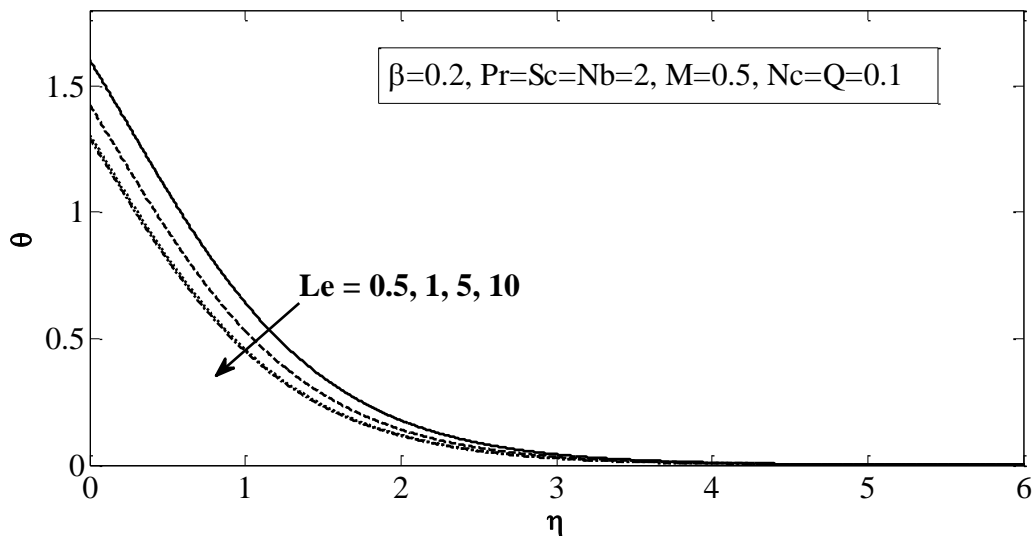


Fig.7 Nanoparticle volume fraction for different values of Le

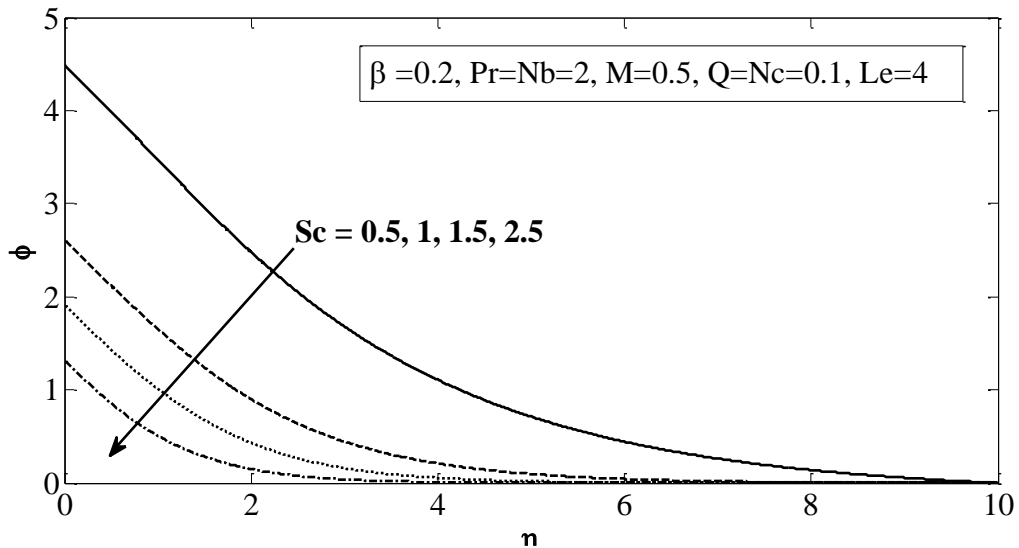


Fig.8 Nanoparticle volume fraction for different values of Sc

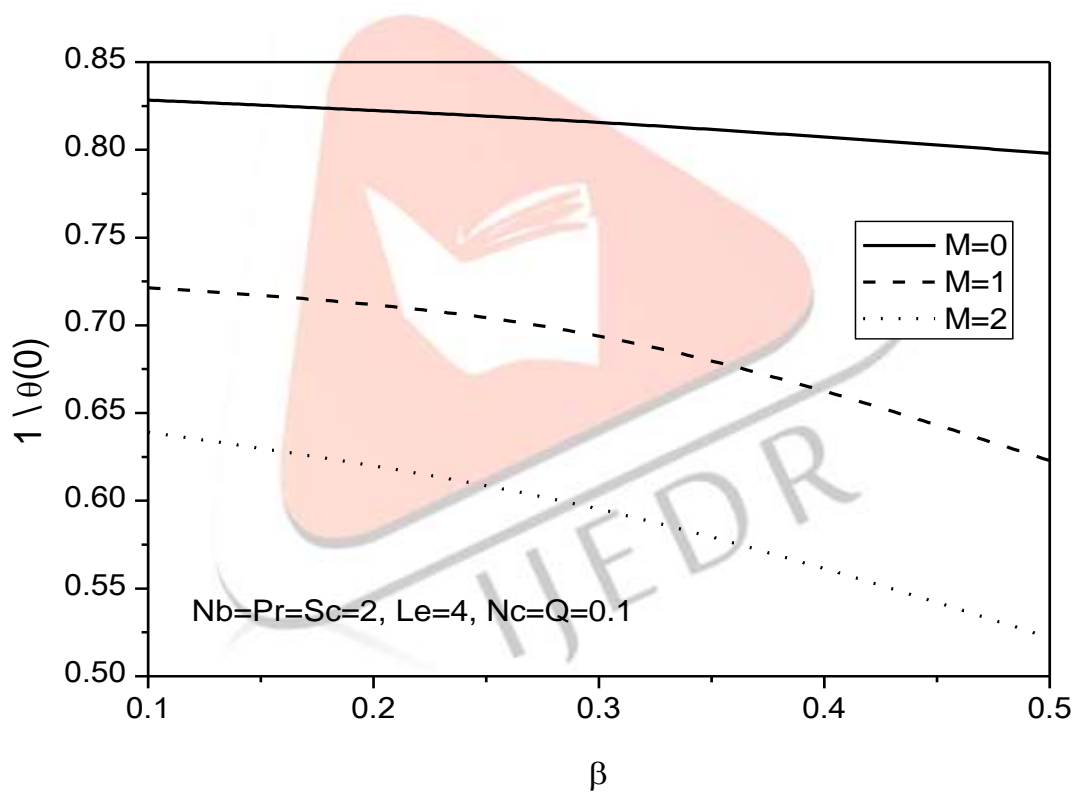


Fig.9(a) Effect of M and β on the reduced local Nusselt number

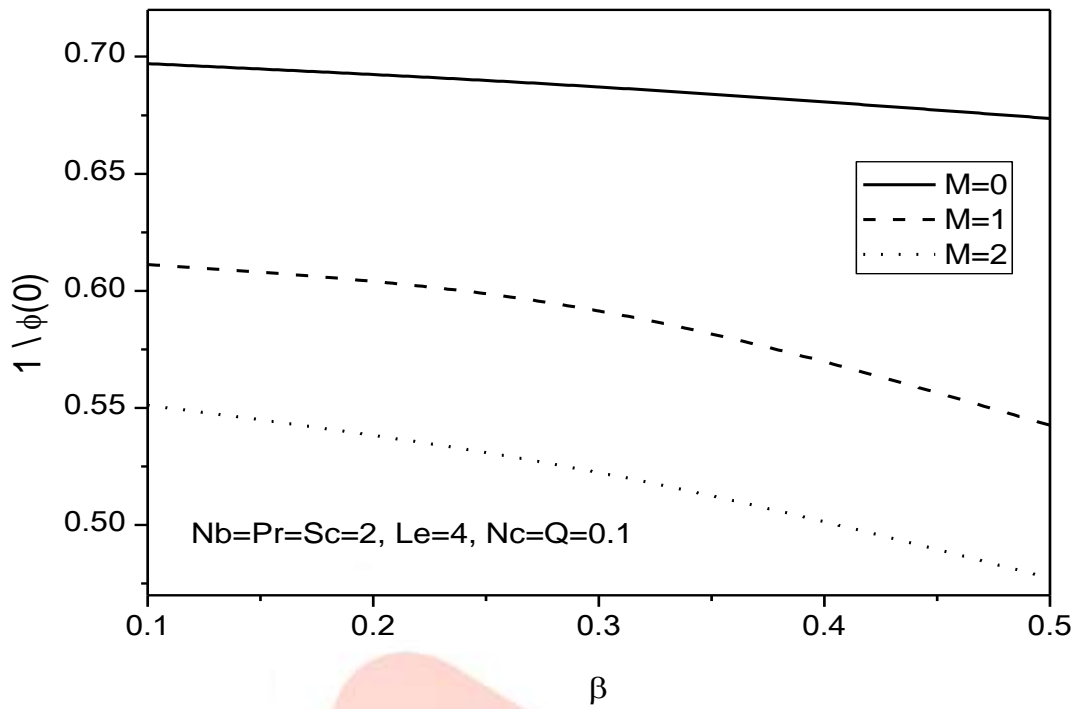


Fig.9(b) Effect of M and β on the local Sherwood number

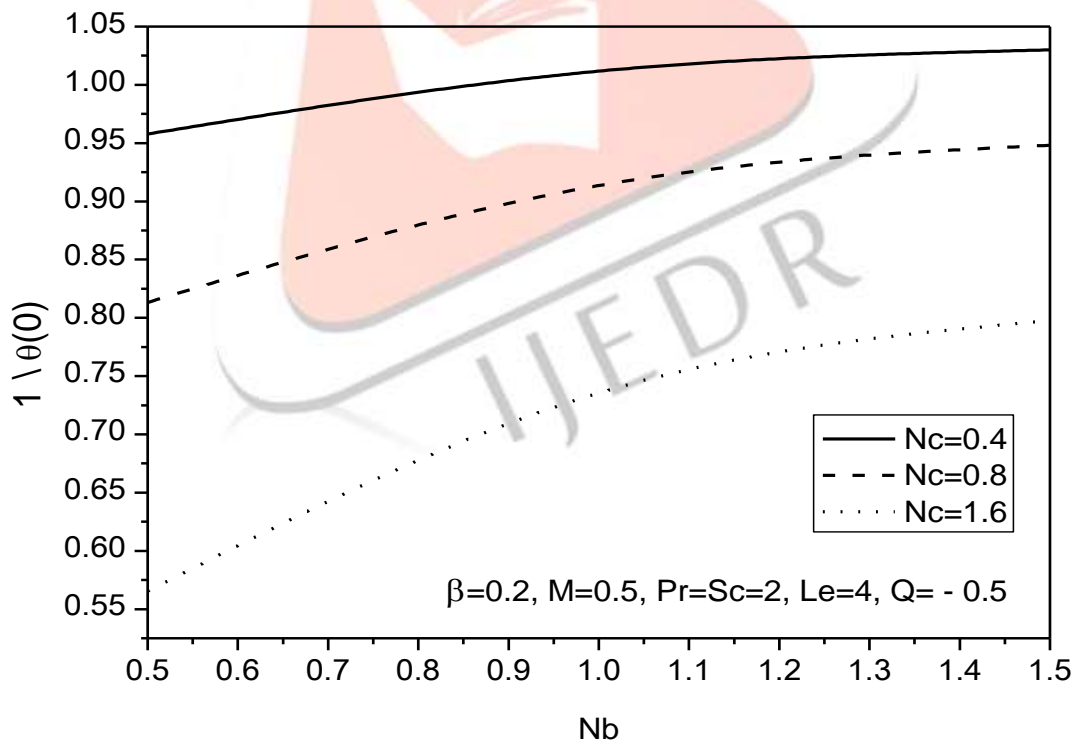


Fig.10(a) Effect of Nb and Nc on the local Nusselt number

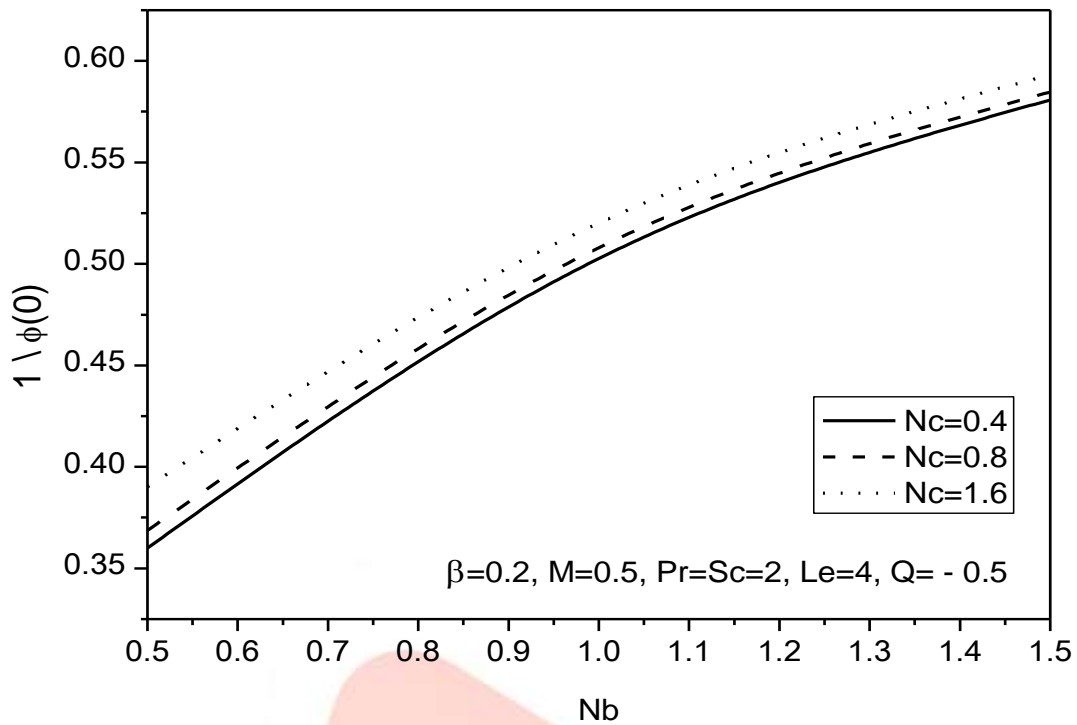


Fig.10(b) Effect of N_b and N_c on the reduced Sherwood number

Table 1 Comparison for viscous case $-\theta'(0)$ with Pr for $\beta = N_c = N_b = Le = Q = Sc = 0$

Pr	$-\theta'(0)$				
	Present results	Nadeem and Hussain [8]	Khan and Pop [28]	Golra and Sidawi [29]	Wang [30]
0.07	0.066000	0.066	0.066	0.066	0.066
0.2	0.169522	0.169	0.169	0.169	0.169
0.7	0.453916	0.454	0.454	0.454	0.454
2.0	0.911358	0.911	0.911	0.911	0.911

REFERENCES

[1] Sakiadis, B. C. (1961). Boundary layer behaviour on continuous solid surfaces: I. The boundary layer equations for two-dimensional and axisymmetric flow. *AICHE J* (7), 26-28.

[2] Stanford Shateyi and JagdishPrakash, (2014), A new numerical approach for MHD laminar boundary layer flow and heat transfer of nanofluids over a moving surface in the presence of thermal radiation, *Boundary Value Problems*, Vol. 2014:2, pp.1-12.

[3] Bhaskar Reddy, N., Poornima, T., and Sreenivasulu, P., (2014), Influence of Variable Thermal Conductivity on MHD Boundary Layer Slip Flow of Ethylene-Glycol Based Cu Nanofluids over a Stretching Sheet with Convective Boundary Condition, *International Journal of Engineering Mathematics*, Vol. 2014, Article ID 905158, pp.1-10.

[4] Swati Mukhopadhyay, Iswar Chandra Mondal, Rama Subba Reddy Gorla, (2013), MHD Flow and Heat Transfer Past a Porous Stretching Non-Isothermal Surface in Porous Medium with Variable Free Stream Temperature, *Thermal Energy and Power Engineering*, Vol. 2, Pages 29-37.

[5] Krishnamurthy, M.R., Prasannakumara, B.C., Giresha, B.J., Rama Subba Reddy Gorla, (2015), Effect of chemical reaction on MHD boundary layer flow and melting heat transfer of Williamson nanofluid in porous medium, *Engineering Science and Technology, an International Journal*, Vol.8,doi:10.1016/j.jestch.2015.06.010.

[6] El-Amin, M.F., (2001), Magnetohydrodynamic free convection and mass transfer flow in micropolar fluid with constant suction, *Journal of Magnetism and Magnetic Materials*, Vol. 234, Issue 3, Pp. 567–574.

[7] Mohammed Ibrahim, S., Gangadhar, K. and Bhaskar Reddy, N., (2015), Radiation and Mass Transfer Effects on MHD Oscillatory Flow in a Channel Filled with Porous Medium in the Presence of Chemical Reaction, *Journal of Applied Fluid Mechanics*, Vol. 8, No. 3, pp. 529- 537.

- [8] Nadeem, S., and Hussain, S. T., (2013), Flow and heat transfer analysis of Williamson nanofluid, *ApplNanosci.*, DOI 10.1007/s13204-013-0282-1.
- [9] Makinde, O.D., (2009), On MHD boundary-layer flow and mass transfer past a vertical plate in a porous medium with constant heat flux, *International Journal of Numerical Methods for Heat & Fluid Flow*, Vol. 19 Iss: 3/4, pp.546 – 554.
- [10] Bachok, Norfifah; Ishak, Anuar, (2009), MHD Stagnation-Point Flow of a Micropolar Fluid with Prescribed Wall Heat Flux, *European Journal of Scientific Research*, Vol. 35 Issue 3, p436.
- [11] Devi, S. P. Anjali; Ganga, B., (2010), Dissipation Effects on MHD Nonlinear Flow and Heat Transfer Past a Porous Surface with Prescribed Heat Flux, *Journal of Applied Fluid Mechanics*; Jan2010, Vol. 3, p1.
- [12] Qasim M, Khan ZH, Khan WA, Ali Shah I., (2014), MHD Boundary Layer Slip Flow and Heat Transfer of Ferrofluid along a Stretching Cylinder with Prescribed Heat Flux, *PLoS ONE*, Vol. 9(1): e83930. doi:10.1371/journal.pone.0083930.
- [13] Das, S., Jana, R. N. and Makinde, O. D., (2014), MHD Boundary Layer Slip Flow and Heat Transfer of Nanofluid Past a Vertical Stretching Sheet with Non-Uniform Heat Generation/Absorption, Vol. 13, No. 03.
- [14] Rajotia, Dinesh and Jat, R. N. (2014), Dual solutions of three dimensional MHD boundary layer flow and heat transfer due to an axisymmetric shrinking sheet with viscous dissipation and heat generation/absorption, *IJPAP*, Vol.52(12), pp.812-820.
- [15] Ahmed M. Megahed, (2015), MHD viscous Casson fluid flow and heat transfer with second-order slip velocity and thermal slip over a permeable stretching sheet in the presence of internal heat generation/absorption and thermal radiation, *The European Physical Journal Plus*, Vol.130:81, pp.1-17.
- [16] Mohamed Abd El-Aziz and Tamer Nabil, (2015), Effect of time-dependent heat source/sink on slip flow and heat transfer from a stretching surface with homotopy analysis method, *Meccanica*, Vol. 50, pp 1467-1480.
- [17] Hunegnaw Dessie, Naikoti Kishan, (2014), MHD effects on heat transfer over stretching sheet embedded in porous medium with variable viscosity, viscous dissipation and heat source/sink, *Ain Shams Engineering Journal*, Vol. 5, Issue 3, Pp.967–977.
- [18] Hitesh Kumar (2013), Heat transfer in mhd boundary-layer flow through a porous medium, due to a non-isothermal stretching sheet, with suction, radiation, and heat annihilation, *Chemical Engineering Communications*, Vol. 200, Issue 7, pp. 895-906.
- [19] Basiri Parsa, A., Rashidi, M.M., and Hayat, T., (2013), MHD boundary-layer flow over a stretching surface with internal heat generation or absorption, *Heat Transfer-Asian Research*, Vol 42, Issue 6, pp. 500–514.
- [20] El-Amin, M.F., (2004), Combined effect of internal heat generation and magnetic field on free convection and mass transfer flow in a micropolar fluid with constant suction, *Materials*, Vol.270, Issues 1–2, Pages 130–135.
- [21] Rajesh Sharma, R. Bhargava, Singh I.V., (2010), Combined effect of magnetic field and heat absorption on unsteady free convection and heat transfer flow in a micropolar fluid past a semi-infinite moving plate with viscous dissipation using element free Galerkin method, *Applied Mathematics and Computation*, Vol.217, Issue 1, Pages 308–321.
- [22] Takhar, H. S., Ram, P. C., Singh, S. S., (1992), Hall effects on heat and mass transfer flow with variable suction and heat generation, *Astrophysics and Space Science*, May 1992, Volume 191, Issue 1, pp 101-106
- [23] Ali J. Chamkha, (2011), Heat and Mass Transfer from MHD Flow over a Moving Permeable Cylinder with Heat Generation or Absorption and Chemical Reaction, *Communications in Numerical Analysis*, Vol.2011, pp.1-20.
- [24] Kinyanjui, M., Kwanza, J.K., and Uppal, S.M., (2001), Magnetohydrodynamic free convection heat and mass transfer of a heat generating fluid past an impulsively started infinite vertical porous plate with Hall current and radiation absorption, *Energy Conversion and Management*, Vol.42(8), pp.917-931.
- [25] Gangadhar, K., (2012), similarity solution for natural convection over a moving vertical plate with internal heat generation and viscous dissipation, *Int. J. of Appl. Math and Mech.*, Vol.8 (18): pp.90-100.
- [26] Gangadhar, K., (2015), Radiation, Heat Generation and Viscous Dissipation Effects on MHD Boundary Layer Flow for the Blasius and Sakiadis Flows with a Convective Surface Boundary Condition, *Journal of Applied Fluid Mechanics*, Vol. 8, No. 3, pp. 559-570.
- [27] Dapra, Scarpi G., (2007), Perturbation solution for pulsatile flow of a non-Newtonian Williamson fluid in a rock fracture, *Int J Rock Mech Min Sci.*, Vol.44, pp.271-278.
- [28] Khan, W.A., and Pop, I., (2010), Boundary-layer flow of a nanofluid past a stretching sheet, *Int J Heat Mass Transf*, Vol. 53, pp.2477-2483.
- [29] Gorla, R.S.R., and Sidawi, I., (1994), Free convection on a vertical stretching surface with suction and blowing, *ApplSci Res*, Vol.52, pp.247-257.
- [30] Wang, Y., (1989), Free convection on a vertical stretching surface, *J Appl Math Mech.*, Vol.69, pp.418-420.